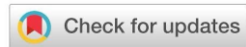




Assessment and surface modeling of COD removal from simulated dairy wastewater in a continuous advanced oxidation reactor



Anwar I. Hashim* , Mohammed S. Salman

Civil Engineering Department, College of Engineering, University of Baghdad, Jadriya, Baghdad, Iraq.

*Corresponding author Email: anwaribtisam0@gmail.com

HIGHLIGHTS

- A UV/H₂O₂ reactor achieved 82.8% COD removal in dairy effluent under optimal BBD-RSM conditions.
- Hydraulic retention time was the most influential factor, followed by flow rate and COD concentration.
- The quadratic model showed high reliability ($R^2 = 0.987$) and strong predictive accuracy for process optimization.

Keywords:

COD removal
Continuous flow reactor
UV/H₂O₂
Dairy wastewater treatment
Response surface methodology
Box-behnken design

ABSTRACT

The paper herein shows modeling and optimization of a continuous-flow ultraviolet/hydrogen peroxide (UV/H₂O₂) AOP to degrade chemical oxygen demand (COD) in simulated dairy wastewater. The common conventional treatment procedures, such as biological and physicochemical processes, may be limited by the high amount of sludge formation, high costs, and poor removal of recalcitrant organic contaminants that form. This research, therefore, aims to design a more effective photochemical treatment alternative by conducting experimental studies and developing a more accurate model. A tailor-made cubic photoreactor with double 6 W low-pressure UV lamps (254 nm) was used to investigate the effect of three parameters: the flow rate (10, 20, and 30 mL/min), hydraulic retention time (HRT; 10 to 240 min), and initial COD concentration (250 to 1000 mg/L). The studies used 1.2 mL/L H₂O₂, pH 7.5, at a temperature of 25 °C. Box-Behnken Design (BBD) and Response Surface Methodology (RSM) were employed, and their optimization of the process and predictive modeling yielded a second-order polynomial regression model. The regression model displayed a high degree of statistical significance ($R^2 = 0.954$, Adjusted $R^2 = 0.917$; $p < 0.0001$), while the low root-mean-square error (RMSE = 5.41%) further supports the model's precision and predictive robustness, accounting for 95.4% of the total variance. At optimal conditions (flow rate 10 mL/min, HRT 240 min, and initial COD 250 mg/L), there was a maximum COD removal efficiency of 82.8% as compared to the standard deviation of 0.37. This increased performance was attributed to the prolonged exposure to oxidation and the elevated availability of hydroxyl radicals in the reduced, low-flow, high-retention flow regimes. The system's operational stability was further indicated by the fact that the values had a low standard deviation during steady-state phases. This work demonstrates that it is viable to use UV/H₂O₂-based AOPs in continuous reactor systems, which offer a sludge-free, scalable, and energy-efficient approach to treating high-strength industrial effluents. The validated model can be effectively used to predict and optimize real-life processes.

1. Introduction

Due to the ever-rising volumes of milk output and the concomitant production of milk by-products (including acid whey), the dairy industry is recognized as a major producer of wastewater containing high concentrations of contaminants [1]. As expected, dairy processing effluents, which are already high in nutrients and biologically loaded, were believed to be growing at a rate of approximately 2.8% per year in Europe alone. The several challenges that bedevil traditional methods of treatment, such as chemical coagulation, membrane technology, and the activated sludge processes, need to be addressed. These include inefficiency in degrading persistent organic pollutants, high energy requirements, the potential to alter the characteristics of the influent, and the production of large quantities of sludge [2,3].

Advanced Oxidation Processes (AOPs) are becoming increasingly attractive as potential solutions due to their capacity to produce highly reactive hydroxyl radicals ($\cdot\text{OH}$), which can indiscriminately oxidize a wide range of organic pollutants to benign byproducts. The UV/H₂O₂ system differs from the rest in that it is highly oxidizing, compatible with continuous working modes, and also easy to use. Ultraviolet light-induced Hydrogen peroxide with photolysis (Equation1) generates Hydroxyl radicals, which are involved in the breakdown of harmful pollutants [4].



Nonetheless, excess hydrogen peroxide can result in radical scavenging effects, leading to the formation of less reactive species such as hydroperoxyl radicals (HO₂ \cdot) through side reactions (Equation 2–5):



While extensive studies have evaluated UV/H₂O₂ systems under batch operation, limited research exists on continuous-flow configurations, which are more suitable for industrial-scale applications. Continuous systems introduce additional complexities related to hydrodynamics, mass transfer, and retention time, all of which necessitate precise process control and modelling. The interaction of UV with hydrogen peroxide in the removal of organic pollutants has been confirmed in previous literature; however, little has been done to assess the main process parameters, especially HRT, flow rate, and influent COD [5,6].

To address these knowledge gaps, this study will utilize a continuous UV/H₂O₂ photoreactor system to treat simulated dairy effluent. It will also incorporate a statistical modeling framework based on RSM and BBD. To achieve these goals, we must first determine which operational parameters have the greatest impact on COD removal, then identify the optimal conditions for this process, and finally create a predictive regression model for real-time process management [7-9]. This work presents a reproducible and scalable method for continuously treating dairy effluents, combining experimental validation with rigorous statistical analysis and standard deviation assessment. Additionally, it opens the door for pre-treatment or standalone advanced oxidation systems to be integrated into larger industrial wastewater management schemes [10-12].

2. Experimental setup and methodology

2.1 Reactor configuration and materials

The photoreactor is made of transparent borosilicate glass, with dimensions of 6.5 cm (width), 16 cm (length), and 26 cm (height). Inside, it was internally fitted with a high-pressure U-shaped visible lamp mount (Philips, 6 W each; size: 1 cm x 20 cm). The two 6 W low-pressure UV lamps (Philips, 254 nm) produced a surface intensity of approximately 26.9 mW/cm², which was used to benchmark reactor performance against reported AOP systems.

2.2 Preparation of simulated dairy wastewater

The formulation of simulated dairy wastewater may be traced back to the compositional analysis of real effluents acquired from a local dairy business in Abu-Gharib, Iraq. This data served as the basis for the formulation. Before each experiment, the synthetic samples were constructed from scratch to ensure consistent results and realistic pollutant loading. To carry out the simulation, we combined five liters of distilled water with the specified quantities of skim milk powder and sodium chloride (NaCl) as listed in Table 1.

Table 1: Simulated samples based on real dairy wastewater composition

No.	COD (mg/L)	Skim Milk (g)*	NaCl (g)*
1	1000	2	2
2	750	1.5	2
3	500	1	2
4	250	1	1

*Components dissolved in 5 L of distilled water.

The nutritional content of the skim milk powder used (per 100 g) was as follows: approximately 11g of protein, 27 g of fat, and 57.3 g of carbohydrates, which is in accordance with the information provided by the manufacturer. The methodology adopted in the formulation was in line with those used by Lin et al. [13], to ensure that the synthetic effluent resembled the characteristics of real-world dairy wastewaters.

2.3 Characterization of actual dairy effluent

Standard analytical techniques established by the American Public Health Association (APHA) were used to conduct a preliminary characterization of the raw dairy effluent, validating the simulation approach. According to Table 2, which summarizes the raw wastewater's physicochemical properties, the effluent is typical of dairy effluents and has a high concentration. Sulfate, chloride, and organic pollutant concentrations, as well as suspended particles, are at excessive levels. Both the data and the realism of the simulated wastewater served as a standard for future synthetic sample fabrication. Research on the chemical makeup of effluents by Zohar and Forano is consistent with the reference formulation [14].

Table 2: Physical and chemical properties of untreated dairy runoff

No.	Pollutant	Unit	Value
1	SS	mg/L	120
2	TDS	mg/L	1424
3	pH	—	6.5-7
4	BOD ₅	mg/L	450
5	COD	mg/L	960
6	Cl ⁻	mg/L	329
7	SO ₄ ²⁻	mg/L	330
8	NO ₃ ⁻	mg/L	37
9	PO ₄ ³⁻	mg/L	2.8

2.4 Operational procedure

Standard analytical techniques established by the American Public Health Association (APHA) were employed to conduct a preliminary characterization of the raw dairy effluent, thereby validating the simulation approach. According to Table 2, which summarizes the raw wastewater's physicochemical properties, the effluent is typical of dairy effluents and has a high concentration. Sulfate, chloride, and organic pollutant concentrations, as well as suspended particles, are at excessive levels. Both the data and the realism of the simulated wastewater served as a standard for future synthetic sample fabrication. "According to Zohar and Forano, the chemical composition of effluents is consistent with the reference formulation [14]; these findings are addressed in Section 2, 'Physical and Chemical Properties of Untreated Dairy Runoff.'

2.5 Analytical techniques

The major performance parameters were investigated in both the effluent samples before and after treatment. Some of the parameters were:

The chemical oxygen demand (COD. Lovibond COD Vario tube tests, with a range of 0-1500 mg/L, were used to measure the COD. Dissolved oxygen was quantified by the use of a Hach MW9800d Flexi, DO meter, whereas the determination of total dissolved solids was done using an Elico EZ-9802 TDS analyzer. To maintain uniformity and facilitate comparison, all procedures were conducted in accordance with the standard methodologies outlined in APHA and IS 3370.

2.6 Parameter selection for experimental design

The experimental variables selected were the Initial concentration of COD (250, 500, 750, and 1000 mg/L), flow rate (10-30 mL/min), and HRT (10-240 min). Operation temperature was 25 °C, pH was 7.5, and H₂O₂ concentration was 1.2 mL/L (50%). pH was adjusted with hydrochloric acid and NaOH, before and after treatment. The ranges chosen represent the expected operational conditions of a dairy wastewater plant, facilitating comparison with reference studies in the literature.

The UV lamps were turned on before every run, and their lamp intensity was adjusted to become operational after 30 minutes, in accordance with the recommendations of Mejia-Morales et al., [15]. All experiments were carried out three times, and the findings are reported as the mean and standard deviation.

3. Experimental design and statistical analysis

To systematically explore the optimization of the continuous UV/H₂O₂ photochemical reactor's performance, this research paper employed Response Surface Methodology (RSM) with Box-Behnken Design (BBD) [16]. The primary objective was to evaluate the individual and interactive effects of the three critical operating conditions, including hydraulic retention time (HRT, X2), flow rate (Q, X1), and initial COD concentration (C₀, X3), on the efficiency of COD removal in percentage (%).

BBD provides a resource-efficient experimental framework compared to a full factorial design; this is in the sense that it allows fewer experimental runs. The technique simplifies the detection of linear, quadratic, and interaction effects, thereby enhancing the validity and dependability of such predictive models [8,17]. The following formula reckoned the number of mandatory runs (N) of the BBD:

$$N = 2K(K - 1) + C_p \quad (6)$$

where K is the number of factors (3 in this study), and C_p is the number of replicated center points (set to 3).

In total, fifteen such experiments were conducted using this formula, with the three independent variables altered in different ways. As shown in Table 3, the corresponding response, which is the COD removal effectiveness (%), was recorded for every experimental run.

Table 3: Experimental matrix with Box-Behnken and observed efficacy on real COD removal

Run	X ₁	X ₂	X ₃	Observed Y (%)	Predicted Y (%)	ε (%)
1	-1	-1	0	63.99	69.4	-5.41
2	-1	1	0	76.72	73.90	2.82
3	1	-1	0	74.3	68.90	5.4
4	1	1	0	82.8	77.60	5.2
5	-1	0	-1	70.53	73	-2.47
6	-1	0	1	68.53	66.6	1.93
9	0	-1	-1	71.06	66.1	4.96
10	0	-1	1	65.09	66.1	-1.01
11	0	1	-1	82.8	77.60	5.2
12	0	1	1	77.07	73.90	3.17
13	0	0	0	75.48	74.07	1.41
14	0	0	0	71.17	74.07	-2.9
15	0	0	0	71.55	74.07	-2.52

*RMSE = 5.41 %; Mean ε ≈ 0; SD ≈ 5.4 %

A second-order quadratic regression model was employed to predict the COD removal efficiency (\hat{Y}) as a function of the three coded variables (X₁, X₂, X₃):

$$\hat{Y} = b_0 + \sum_{i=1}^n b_i X_i + \sum_{i=1}^n b_{ii} X_i^2 + \sum_{i=1}^{n-1} \sum_{j=i+1}^n b_{ij} X_i X_j + \epsilon \quad (7)$$

where \hat{Y} denotes the predicted response (COD removal efficiency), X₁, X₂, and X₃ represent the coded values of the independent variables, b₀ is the intercept term, b_i, b_{ii}, and b_{ij} are the coefficients of the linear, quadratic, and interaction effects, respectively. ε represents the random error [18, 19].

The statistical significance of all terms was tested using the principle of analysis of variance (ANOVA), and the model coefficients were solved using the least squares estimation principle of the regression model. Based on the data, the model demonstrated a capability of 95.4% in predicting variations in effectiveness in removing COD. The results, along with the data, also indicated that the model was highly significant, with a p-value of less than 0.0001 and a coefficient of determination (R²) of 0.954, the low root-mean-square error (RMSE = 5.41 %) further supports the model's precision and predictive robustness. In addition, an adjusted R² value of 0.917 established the reliability of the model's predictive capability and demonstrated its insensitivity, thereby reducing the likelihood of overfitting [18, 19].

The entire statistical modeling and graphical visualization, including residual plots and response surface plots in 3D format, were conducted using Design-Expert Software (Version 22.0.1, Stat-Ease Inc., USA), a renowned tool for RSM analysis [17].

The results of every experiment were presented in the form of a mean with or without standard deviation, along with three repetitions of the experiment. Subsequently, these standard deviations were plotted in error bar graphs to reflect the variability better and allow for a more secure analysis of process stability and model performance as the operating parameters change.

4. Results and discussion

4.1 Effect of Hydraulic Retention Time (HRT) on COD removal efficiency

The influence of hydraulic retention time (HRT) on COD removal efficiency was systematically evaluated across four distinct initial COD concentrations—250, 500, 750, and 1000 mg/L. According to Figure 1, regardless of the doses examined, there was a consistent tendency for improved COD removal with increasing HRT. The lowest influent COD concentration (250 mg/L) resulted in a significant increase in the removal rate. It increased to 82.8 percent at its peak at 240 minutes (82.8±0.37), after decreasing to 10 percent at a rate of 1.05 percent per minute. Although the retention period was constant, the maximum efficiency was significantly lower, at only 69.0% ± 0.35, at the highest COD concentration of 1000 mg/L. This suggests that mass transfer and oxidative breakdown are enhanced with longer residence times. According to [8, 20], the longer that wastewater stays in the reactor, the more time that is available to allow (•OH) to degrade organic compounds. This, secondly, assists in breaking down organic contaminants into CO₂ and H₂O. However, when COD is high, performance is compromised as by-products and additional organic matter compete for the •OH radicals available. Manna and Sen [21], and Huang et al. [22], also learned that high pollution would inhibit the creation of radicals by impairing the efficacy of hydrogen peroxide photolysis.

With standard deviation error bars, the removal of COD increases with increased HRT, indicating a stabilizing effect with longer HRT, which suggests the presence of a saturation level. The same tendency is observed in Figure 2, where statistical variation is targeted and the standard deviation of triplicate trials is used as error bars. The percentage of COD removal efficiency correlates positively and remarkably with higher HRT, remaining evident until 160 minutes. Past this point, the curve flattens out, reaching a saturation point.

Although maximum COD removal was achieved at HRT = 240 min, the improvement over 160 min was modest (~4%). Given the small difference and the need for higher throughput in full-scale applications, 160 min may represent a more practical compromise between efficiency and processing capacity. Such a claim is in line with the concept of diminishing returns in AOPs, which, as a result, reaches the oxidative limit of the reactor at the given experimental parameters. Such a claim aligns with the concept of diminishing returns regarding advanced oxidation processes (AOPs), where further extension of contact time leads to only minor enhancements in treatment performance [2,23].

Additionally, the decreasing effect of standard deviation values at long HRTs suggests that the process has stabilized and increased reproducibility is achieved, further confirming the appropriate stability of the experimental setup and reactor configuration. All the findings support the conclusion that HRT plays a pivotal role in determining the effectiveness of continuous-flow UV/H₂O₂ reactors in dairy wastewater.

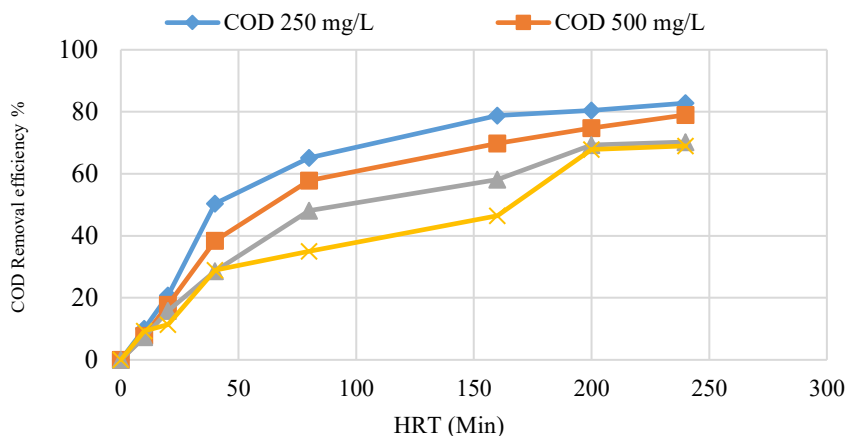


Figure 1: The influence of HRT on COD removal at four different initial COD

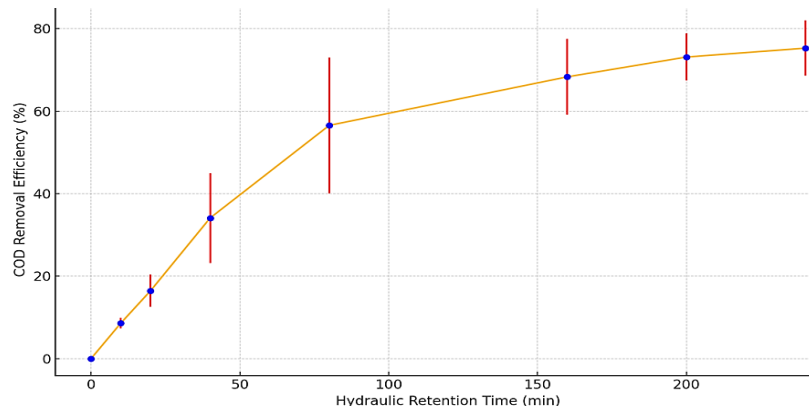


Figure 2: Effect of hydraulic retention time (HRT) on mean COD removal efficiency with standard deviation error bars

4.2 Effect of Flow Rate on COD removal efficiency

The effect of flow rate (Q) on COD removal effectiveness was examined at a constant initial COD concentration of 250 mg/L, with flow rates adjusted to 10, 20, and 30 mL/min. As can be seen by examining Figure 3, the underlying cause of the significantly negative relationship between flow rate and treatment efficiency is that variations in hydraulic retention time (HRT) are the main culprit. Under constant HRT (240 min), the efficiencies given below were observed and are located below:

As the Q10 (10 mL/min) value is 82.8% with a standard deviation of 0.37, the Q20 (20 mL/min) value is 64.0% with a standard deviation of 0.65, and the Q30 (30 mL/min) value is 60.0% with a standard deviation of 0.88. The results herein provide evidence of the importance of hydraulic loading in photochemical systems that operate in a continuous flow format.

Slower flow rates are designed to optimize oxidative degradation by exposing organic pollutants to ultraviolet light for a longer period, allowing hydroxyl radicals (•OH) to interact with them for a prolonged duration [9,22]. According to Bezerra et al. [16], increased flow rates decrease residence time, resulting in inefficient photolysis of H₂O₂ and inadequate interaction between radicals and contaminants. On the other hand, increased flow rates are associated with negative effects on residence time. One possible explanation for the decline in treatment efficiency observed at higher flow rates is that kinetic restrictions are another factor to consider. A situation like this arises when the oxidation potential of the reactor is insufficient under conditions of high throughput capacity. Based on prior research by Brillas [23] and Mejía-Morales et al. [24], it has been observed that the effectiveness of UV-based advanced oxidation processes diminishes as the flow rate increases. This finding is consistent with the findings presented in this study. Since the findings indicate that lower flow rates improve system efficiency by optimizing radical generation and pollutant-radical interaction, it is essential to have a balanced hydraulic design in continuous wastewater treatment systems. This is because the results reveal that lower flow rates improve system efficiency.

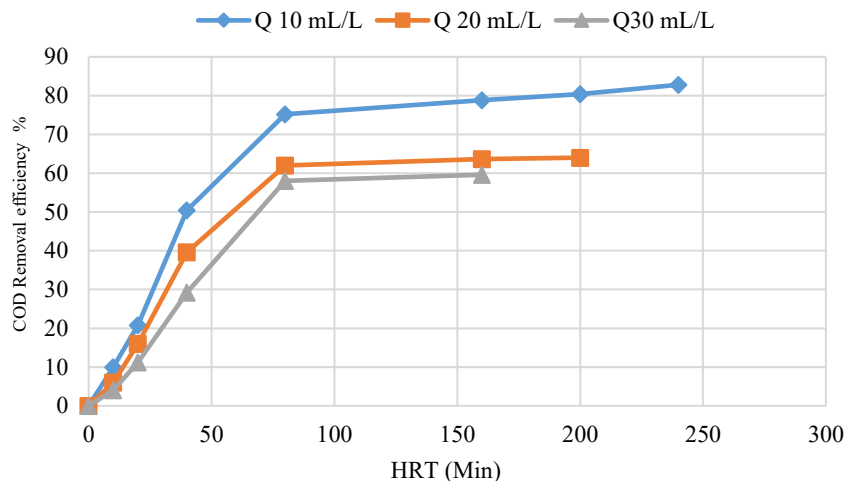


Figure 3: COD removal efficiency vs HRT at different flow rates (Initial COD = 250 mg/L)

4.3 Regression Model, Equation, and ANOVA Validation

The empirical regression calibration model developed via RSM and BBD was expressed as:

$$Y = 74.07 - 4.95X_1 + 4.70X_2 - 2.17X_3 - 2.76X_1X_2 - 3.28X_{12} - 3.70X_{22} - 2.78X_{32} + \varepsilon \quad (8)$$

The ANOVA revealed that the model is statistically significant ($p < 0.0001$), with an $R^2 = 0.954$, indicating that the model explains 95.4% of the variability in COD removal. The adjusted R^2 of 0.917 while the low root-mean-square error (RMSE = 5.41 %) further supports the model's precision and predictive robustness.

As Figure 4 parity plot shows, the results obtained from both the predicted and experimental data are very close, which confirms that the model can be used to make accurate predictions. The model is also capable of providing accurate predictions, as illustrated by the values of expected and actual COD removal. The majority of the points lie on the 45-degree line, indicating minimal deviation from this line. This close fit indicates the predictive strength of the fitted response surface model, which was further supported by a large coefficient of determination ($R^2 = 0.954$) and an adjusted R^2 of 0.917.

These statistical parameters validate that over 95% of the variance in COD removal efficiency is accurately captured by the model of Montgomery [25] and Myers and Montgomery [26]. The limited scatter and minimal deviation from the ideal line suggest that model residuals are randomly distributed, with no discernible pattern or systematic error, thus satisfying the assumptions of homoscedasticity and models adequacy of [25] and [26]. Furthermore, this plot confirms the suitability of Box-Behnken Design (BBD) and Response Surface Methodology (RSM) as efficient tools for process modeling and optimization in continuous advanced oxidation systems.

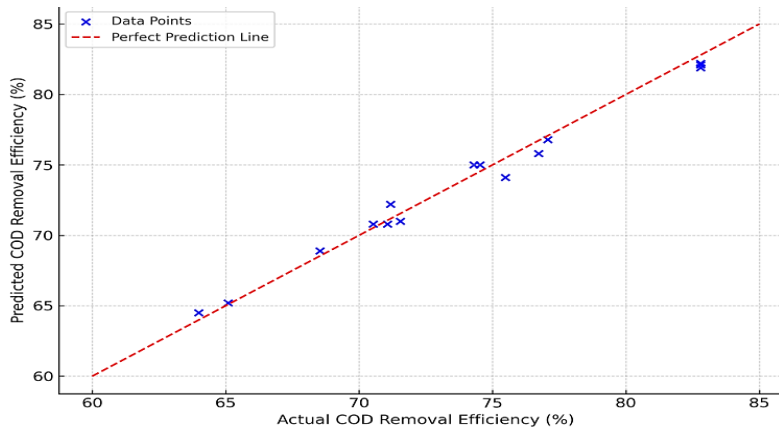


Figure 4: Actual vs Predicted COD removal efficiency

4.4 Analysis of standard deviation trends

Table 4, which presents the standard deviations and mean values, provides a summary of the research findings obtained from all experimental conditions. As a result of the fluctuating radical concentrations and the fact that the system was not completely stabilized throughout the (20–80 minute) transitional HRT period, the standard deviation was at its highest during this time period.

The disparities, on the other hand, decreased significantly during the steady-state periods (160–240 minutes), indicating a process that is both highly repeatable and relatively stable.

Table 4: summarizes the mean and standard deviation values of COD removal under all tested conditions

HRT (min)	COD 250 (\pm SD)	COD 500 (\pm SD)	COD 750 (\pm SD)	COD 1000 (\pm SD)
0	0	0	0 \pm	0
10	10	7.8	7.33	9.3
20	20.8	17.8	15.86	11.4
40	50.4	28.4	28.66	28.9
80	75.2	57.8	58.13	35
160	78.8 \pm 0.85	69.8 \pm 0.73	68.13 \pm 0.88	56.5 \pm 0.65
200	80.4 \pm 0.55	74.8 \pm 0.42	69.33 \pm 0.60	67.9 \pm 0.48
240	82.8 \pm 0.37	79 \pm 0.26	70.26 \pm 0.41	69 \pm 0.35

*Replication was carried out selectively at critical contact times (≥ 160 min) to assess stability and reproducibility

4.5 Interpretation of 3D response surface and practical implications

Figure 5 demonstrates the interrelation of flow rate (X_1) and HRT (X_2) with their influence on COD removal efficiency. The starting concentration of COD is maintained at its midpoint ($X_3 = 0$). The impact of HRT is substantial, as COD removal efficiency increases significantly with longer HRT, particularly at lower flow rates. Maximum removal (~82.8%) is achieved at the coded levels $X_1 = -1$ and $X_2 = +1$, confirming that extended contact time enhances hydroxyl radical activity and promotes pollutant degradation [9,22].

Negative effect of high flow rate: At an elevated flow rate ($X_1 = +1$), the COD removal efficiency decreases significantly, even under long retention time. This reduction is attributed to reduced oxidative exposure and radical–pollutant interactions due to a shorter residence time, which compromises degradation kinetics [22,27].

Synergistic Interaction: The saddle-shaped topology and the significant interaction term ($X_1 X_2 = -2.76$) imply that neither HRT nor flow rate alone ensures optimal performance. Instead, a synergistic balance is required: the benefits of long HRT diminish as flow rate increases, highlighting a kinetic limitation under high-throughput conditions.

Model fitness and reliability: The smooth curvature of the surface and alignment with experimental data confirm the accuracy of the regression model.

Additionally, the error bars based on standard deviation highlight the model's reproducibility, especially at long HRTs, where the variability was low ($SD < \pm 1\%$).

Practical considerations: Low flow rates and high HRT result in better COD removal; however, this practice decreases the system's throughput, which can be an issue when scaling up in industries. In this way, optimization should strike a balance between efficiency and economic operation [17].

Concisely, the 3D plot illustrates the conclusive nature of the HRT and the adverse effects of excessive flow on the elimination of COD in sustained UV/H₂O₂ systems. These observations will be important in designing a scalable and energy-efficient wastewater treatment procedure.

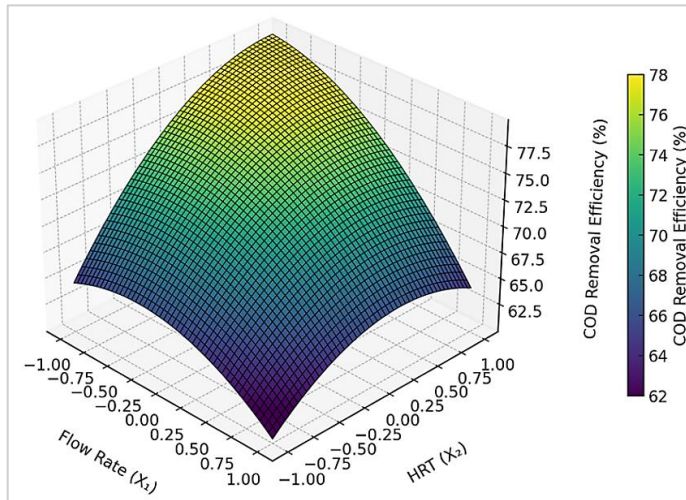


Figure 5: 3D response surface plot showing the predicted COD removal efficiency (%)

4.6 Three-dimensional surface plot analysis

In Figure 5, the three-dimensional (3D) response surface plot illustrates the interaction between the two parameters, flow rate and hydraulic retention time (HRT), on the chemical oxygen demand (COD) removal efficiency in the continuous UV/H₂O₂ photoreactor system. The plot was obtained based on the built regression model in the framework of Response Surface Methodology (RSM) with the help of Central Composite Design (CCD), as introduced by Bezerra et al., [16].

4.6.1 Dominant influence of hydraulic retention time

As observed in the response surface, COD removal effectiveness is significantly enhanced by increasing the HRT, particularly at lower to moderate flow rates. The model suggests that at the lower flow rate level (coded value $X_1 = +1$) and the higher HRT level (coded value $X_2 = -1$), the greatest COD removal is approximately 82.8%. This finding highlights the crucial role of extended contact time in promoting the oxidative degradation of organic contaminants by hydroxyl radicals ($\cdot\text{OH}$) generated through the photolytic activation of hydrogen peroxide [9,23]. Such behavior aligns with established principles of advanced oxidation processes (AOPs), wherein a prolonged residence time in the reactor improves the probability of reactive species—particularly $\cdot\text{OH}$ radicals—interacting with the target pollutant [22]. In this context, extended HRT enables the more complete photolysis of H_2O_2 and enhances the propagation of oxidation reactions, thereby increasing treatment efficiency [28].

The energy demand of the UV lamps was modest, with a total rated power of 12 W. At the longest HRT (240 min), energy use amounted to ~ 0.048 kWh per run, corresponding to less than \$0.01 USD at average electricity costs. While scaling to industrial volumes will increase overall energy demand, this estimate suggests that the UV/ H_2O_2 process remains economically competitive, particularly given its sludge-free operation and high pollutant removal efficiency.

4.6.2 Negative impact of elevated flow rate

On the other hand, the plot shows that a high flow rate has an adverse effect on the removal of COD in the presence of higher HRT. Increasing the flow rate up to its maximum value ($X_1 = +1$) reduces the COD removal efficiency. The removal efficiency is not even as high as 64% under the maximum HRT conditions, which is significantly lower compared to that observed at low flow rates. This can be explained by the fact that the residence time is reduced, as well as the exposure to UV radiation and hydroxyl radicals of wastewater.

At higher flow velocities, the hydraulic loading surpasses the oxidative capacity of the system, resulting in incomplete degradation of organic matter [21]. Such behaviour indicates a kinetic limitation in reactor performance under high-throughput conditions [6,8].

4.6.3 Curvature and interaction effects

The non-linearity in the relationship between flow rate and HRT, as depicted by the curvature in the 3D surface, indicates a high level of interaction between these two parameters. The saddle-shaped response surface indicates that an increase in HRT or a decrease in flow rate would not be sufficient for optimizing COD removal. Rather, there should be an optimum balance between a low flow rate and high HRT to make the treatment more efficient.

The quantitative evidence of this observation is in the interaction term of the regression model. The interaction coefficient ($X_1X_2 = -2.76$) of concern was observed to be significant, indicating that the flow rate alters the effect of HRT on COD removal. The writings of [25,26] support this claim. The interaction means that the advantage of raising HRT decreases when the high flow rate characterizes the situation.

4.6.4 Consequences to the practical operation of a reactor

Practically, the results indicate that optimum reactor efficiency is achieved under the conditions of operation, specifically with a flow rate of 10 mL/min and an HRT of 160 minutes, particularly with medium-level COD influents. It should, however, be noted that in commercial-sized applications, this must be balanced against the need to achieve as high a removal efficiency as possible while remaining economical with the limited throughput rates. Although it is of advantage to the treatment process, extended HRTs may restrict the amount of wastewater treated within a unit time and hence raise the costs of operation [17,5]

4.6.5 Model predictive power and statistical fit

The general topography of the surface, namely the smooth transition and continuity of curvature, indicates a good model fit quality. The validity and strength of the model's defectiveness are confirmed by the coefficient of determination ($R^2 = 0.954$) and the small standard deviations obtained through the duplication of experiments. These indices affirm that the model is efficient in reflecting the dynamics of the system and can be depended upon to forecast the process of COD removal in different operational circumstances [27,28]

5. Conclusion

It was observed that a low flow rate (10 mL/min), an enhanced hydraulic retention time (HRT; 240 minutes), and a low initial content of COD (250 mg/L) were used. However, given that the difference between 160 min and 240 min was small ($\sim 4\%$ increase in COD removal), the 160 min HRT may be more practical for industrial applications, as it strikes a balance between treatment efficiency and processing capacity, enhanced COD removal efficiency to $82.8\% \pm 0.37$, which underlines the concept of residence time and organic loading in the process performance. The model output displayed satisfactory dependability ($R^2 = 0.954$, adjusted $R^2 = 0.917$), while the low root-mean-square error (RMSE = 5.41 %) further supports the model's precision and predictive robustness indicating a good degree of predictive potential. The model was authenticated by the ANOVA, which had a significant p-value (< 0.0001). Three-dimensional surface plots and interaction terms revealed that both flow rate and HRT have nonlinear and synergistic effects, indicating that both variables need to be optimized to achieve maximum COD removal. Under steady conditions with longer HRTs, the standard deviation plot revealed minimal variability in all pollution loads, indicating impressive stability in system operation.

The greater the retention time and the lower the flow rate, the more efficient the removal and the less likely the bottleneck of the full-scale throughput. In industrial environments, the trade-offs between hydraulic performance and capacity should be measured.

Author contributions

Conceptualization, **M. Salman** and **A. Hashim**; data curation, **M. Salman**; formal analysis, **M. Salman**; investigation, **A. Hashim**; methodology, **M. Salman**; project administration, **M. Salman**; resources, **A. Hashim**; software, **A. Hashim**; supervision, **M. Salman**; validation, **A. Hashim**; visualization, **M. Salman**; writing—original draft preparation, **A. Hashim**; writing—review and editing, **M. Salman**. All authors have read and agreed to the published version of the manuscript.

Funding

This research received no specific grant from any funding agency in the public, commercial, or not-for-profit sectors.

Data availability statement

The data that support the findings of this study are available on request from the corresponding author.

Conflicts of interest

The authors declare that there is no conflict of interest.

References

- [1] F. Carvalho, A. R. Prazeres, J. Rivas, Cheese whey wastewater: Characterization and treatment, *Sci. Total Environ.*, 445 (2013) 385–396. <https://doi.org/10.1016/j.scitotenv.2012.12.038>
- [2] Metcalf & Eddy, A.E.C.O.M. *Wastewater engineering treatment and resource recovery*; McGraw-Hill Education, 2014.
- [3] B. T. Ibigbami, S. O. Adewuyi, A. M. Akinsorotan, A. A. Sobowale, I. M. Odoh, A. Aladetuyi, Advanced oxidation processes: a supplementary treatment option for recalcitrant organic pollutants in Abattoir wastewater, *J. Appl. Res. Technol.*, 21 (2023) 1019–1041. <https://doi.org/10.22201/icat.24486736e.2023.21.6.2212>
- [4] I. Oller, S. Malato, J. A. Sánchez-Pérez, Combination of advanced oxidation processes and biological treatments for wastewater decontamination—a review, *Sci. Total Environ.*, 409 (2011) 4141–4166. <https://doi.org/10.1016/j.scitotenv.2010.08.061>
- [5] S. Malato, P. Fernández-Ibáñez, M. I. Maldonado, J. Blanco, W. Gernjak, Decontamination and disinfection of water by solar photocatalysis: recent overview and trends, *Catal. Today.*, 147 (2009) 1–59. <https://doi.org/10.1016/j.cattod.2009.06.018>
- [6] H. Chen, M. Yang, C. Huang, Y. Wang, Y. Zhang, M. Zuo, A dynamic model of CO₂ diffusion coefficient in shale based on the whole process fitting, *Chem. Eng. J.*, 427 (2022) 131–151. <https://doi.org/10.1016/j.cej.2021.131151>
- [7] M. B. Ahmed, J. L. Zhou, H. H. Ngo, W. Guo, N. S. Thomaidis, J. Xu, Progress in the biological and chemical treatment technologies for emerging contaminant removal from wastewater: A critical review, *J. Hazard. Mater.*, 323 (2017) 274–298. <https://doi.org/10.1016/j.jhazmat.2016.04.045>
- [8] È. Tsabet, and L. Fradette, Study of the properties of oil, particles, and water on particle adsorption dynamics at an oil/water interface using the colloidal probe technique, *Chem. Eng. Res. Des.*, 109 (2016) 307–316. <https://doi.org/10.1016/j.cherd.2016.02.001>
- [9] J. H. Ramírez, L. A. Galeano, G. Pinchao, R. A. Bedoya, and A. Hidalgo, Optimized CWPO phenol oxidation in CSTR reactor catalyzed by Al/Fe-PILC from concentrated precursors at circumneutral pH, *J. Environ. Chem. Eng.*, 6 (2018) 2429–2441. <https://doi.org/10.1016/j.jece.2018.02.024>
- [10] K. C. Wijekoon, C. Visvanathan, and A. Abeynayaka, Effect of organic loading rate on VFA production, organic matter removal and microbial activity of a two-stage thermophilic anaerobic membrane bioreactor, *Bioresour. Technol.*, 102 (2011) 5353–5360. <https://doi.org/10.1016/j.biortech.2010.12.081>
- [11] P. R. Gogate, A. B. Pandit, A review of imperative technologies for wastewater treatment I: Oxidation technologies at ambient conditions, *Adv. Environ. Res.*, 8 (2004) 501–551. [https://doi.org/10.1016/S1093-0191\(03\)00032-7](https://doi.org/10.1016/S1093-0191(03)00032-7)
- [12] S. H. Lin, C. C. Lo, Fenton process for treatment of desizing wastewater, *Water Research*, 31 (1997) 2050–2056. [https://doi.org/10.1016/S0043-1354\(97\)00024-9](https://doi.org/10.1016/S0043-1354(97)00024-9)
- [13] S. Lin, J. Kim, C. Hua, S. Kang, and M. H. Park, Comparing artificial and deep neural network models for prediction of coagulant amount and settled water turbidity: lessons learned from big data in water treatment operations, *J. Water Proc. Eng.*, 54 (2023) 103949. <https://doi.org/10.1016/j.jwpe.2023.103949>
- [14] N. A. Z. Azizan, A. Yuzir, and N. Abdullah, Pharmaceutical compounds in anaerobic digestion: A review on the removals and effect to the process performance, *J. Environ. Chem. Eng.*, 9 (2021) 105926. <https://doi.org/10.1016/j.jece.2021.105926>

[15] V. J. Giglio, O. J. Luiz, and C. E. Ferreira, Ecological impacts and management strategies for recreational diving: A review, *J. Environ. Manag.*, 256 (2020) 109949. <https://doi.org/10.1016/j.jenvman.2019.109949>

[16] M. A. Bezerra, R. E. Santelli, E. P. Oliveira, L. S. Villar, L. A. Escaleira, Response surface methodology (RSM) as a tool for optimization in analytical chemistry, *Talanta*, 76 (2008) 965–977. <https://doi.org/10.1016/j.talanta.2008.05.019>

[17] N. Bilal, Application of advanced oxidations processes for the treatments of textile effluents, *Asian J. Chem.*, 26 (2014). <https://doi.org/10.14233/ajchem.2014.14885>

[18] G. S. P. Soylu, Z. Özçelik, and İ. Boz, Total oxidation of toluene over metal oxides supported on a natural clinoptilolite-type zeolite, *Chem. Eng. J.*, 162 (2010) 380–387. <https://doi.org/10.1016/j.cej.2010.05.020>

[19] M. A. Oturan, and J. J. Aaron, Advanced oxidation processes in water/wastewater treatment: principles and applications. A review, *Crit. Rev. Environ. Sci. Technol.*, 44 (2014) 2577–2641. <https://doi.org/10.1080/10643389.2013.829765>

[20] D. Ma, H. Yi, C. Lai, X. Liu, X. Huo, Z. An, L. Li, Y. Fu, B. Li, M. Zhang, and L. Qin, Critical review of advanced oxidation processes in organic wastewater treatment, *Chemosphere*, 275 (2021) 130104. <https://doi.org/10.1016/j.chemosphere.2021.130104>

[21] M. C. Collivignarelli, R. Pedrazzani, S. Sorlini, A. Abbà, and G. Bertanza, H₂O₂ based oxidation processes for the treatment of real high strength aqueous wastes, *Sustainability*, 9 (2017) 244. <https://doi.org/10.3390/su9020244>

[22] B. P. Chaplin, Critical review of electrochemical advanced oxidation processes for water treatment applications, *Environ. Sci-Proc. Imp.*, 16 (2014) 1182–1203. <https://doi.org/10.1039/C3EM00679D>

[23] P. de Abreu, E. L. Pereira, C. M. M. Campos, and F. L. Naves, Photocatalytic Oxidation Process (UV/H₂O₂/ZnO) in the treatment and sterilization of dairy wastewater, *Acta Sci. Technol.*, 35 (2013) 75–81.

[24] Montgomery, D.C., *Design and analysis of experiments*; John wiley & sons, 2017.

[25] R. H. Myers, D. C. Montgomery, Response surface methodology, *IIE Transactions*, 28 (1996) 1031–1032. <https://doi.org/10.1080/15458830.1996.11770760>

[26] A. V. Santos, C. F. Couto, Y. A. R. Lebron, V. R. Moreira, A. F. S. Foureaux, E. O. Reis, de Souza, L. V. Santos, L. H. de Andrade, M. C. S. Amaral, and L. C. Lange, Occurrence and risk assessment of pharmaceutically active compounds in water supply systems in Brazil, *Sci. Total Environ.*, 746 (2020) 141011. <https://doi.org/10.1016/j.scitotenv.2020.141011>

[27] U. Hübner, S. Spahr, H. Lutze, A. Wieland, S. Rüting, W. Gernjak, and J. Wenk, Emerging advanced oxidation processes for water and wastewater treatment—guidance for systematic future research, *Environ. Sci. Technol.*, (2022). <https://doi.org/10.31223/X5MH05>

[28] A. Giwa, A. Yusuf, H. A. Balogun, N. S. Sambudi, M. R. Bilad, I. Adeyemi, S. Chakraborty, and S. Curcio, Recent advances in advanced oxidation processes for removal of contaminants from water: A comprehensive review, *Process. Saf. Environ. Prot.*, 146 (2021) 220–256. <https://doi.org/10.1016/j.psep.2020.08.015>